

A. L. Huber · M. Heuer · K. T. Fehr · K. Bente
E. Schmidbauer · G. D. Bromiley

Characterization of synthetic hedenbergite (CaFeSi₂O₆)–petedunnite (CaZnSi₂O₆) solid solution series by X-ray powder diffraction and ⁵⁷Fe Mössbauer spectroscopy

Received: 28 October 2002 / Accepted: 23 January 2003

Abstract Clinopyroxenes along the solid solution series hedenbergite (CaFeSi₂O₆)–petedunnite (CaZnSi₂O₆) were synthesized under hydrothermal conditions and different oxygen fugacities at temperatures of 700 to 1200 °C and pressures of 0.2 to 2.5 GPa. Properties were determined by means of X-ray diffraction, electron microprobe analysis and ⁵⁷Fe Mössbauer spectroscopy at 298 K. Unit-cell parameters display a linear dependency with changing composition. Parameters *a*₀ and *b*₀ exhibit a linear decrease with increasing Zn content while the monoclinic angle *β* increases linearly. Parameter *c*₀ is not affected by composition and remains constant at a value of 5.248 Å. The molar volume can be described according to the equation $V_{\text{mol}} (\text{ccm mol}^{-1}) = 33.963(16) - 0.544(31) \cdot \text{Zn pfu}$. The isomer shifts of ferrous iron on the octahedral M1 site in hedenbergite are not affected by composition along the hedenbergite–petedunnite solid solution series and remain constant at an average value of 1.18 mm s⁻¹. Quadrupole splittings of Fe²⁺ on the M1 are, however, strongly affected by composition, and they decrease linearly with increasing petedunnite component in hedenbergite, ranging from 2.25 mm s⁻¹ for pure hedenbergite end member to 1.99 mm s⁻¹ for a solid

solution containing 84 mole% petedunnite. The half-widths of intermediate solid solutions vary between 0.26 and 0.33 mm s⁻¹, indicating, in accordance with the microprobe analyses and X-ray diffraction, that samples are homogeneous and well-crystallized. The data from this study demonstrate that the crystallinity of hedenbergitic clinopyroxenes can be improved by using oxide mixtures as starting materials. Crystal sizes for intermediate compositions range up to 70 μm, suitable for standard single-crystal X-ray analysis.

Keywords Petedunnite · Hedenbergite · Solid solution · Synthesis · Crystal chemistry · Moessbauer spectroscopy · Unit-cell parameter · Clinopyroxene

Introduction

Hedenbergite (CaFe²⁺Si₂O₆) and petedunnite (CaZnSi₂O₆) are chain silicates belonging to the group of clinopyroxenes, crystallizing in the monoclinic space group *C2/c*. Ca occupies the distorted eight-fold-coordinated M2 polyhedra, whereas Fe²⁺ and Zn²⁺ occupy the regular six fold-coordinated M1 octahedra in hedenbergite and petedunnite, respectively. The structures of end members hedenbergite and petedunnite were refined by Clark et al. (1969) and Ohashi et al. (1996), respectively. Hydrothermal synthesis of hedenbergite was performed by Nolan (1969), Rutstein and Yund (1969), Turnock et al. (1973), Gustafson (1974), Kinrade et al. (1975), Burton et al. (1982), Haselton et al. (1987), Moecher and Chou (1990), Raudsepp et al. (1990), Perkins and Vielzeuf (1992), Kawasaki and Ito (1994), Zhang et al. (1997) and Redhammer et al. (2000). The stability of hedenbergite at 0.2 GPa as a function of temperature and oxygen fugacity was determined by Gustafson (1974) and Burton et al. (1982). Naturally occurring petedunnite was first described by Essene and Peacor (1987) from Zn skarns in Franklin, New Jersey. Petedunnite occurs as a major component in quaternary solid solution with hedenbergite, johannsenite (CaMnSi₂O₆) and diopside

This paper is dedicated to Prof. Dr. Georg Amthauer, Salzburg, on occasion of his 60th birthday

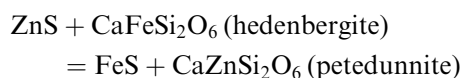
A. L. Huber · K. T. Fehr (✉) · E. Schmidbauer
Department of Earth- and Environmental Sciences,
Ludwig-Maximilians University Munich,
Theresienstr.41, 80333 Munich, Germany
e-mail: fehr@petrol.min.uni-muenchen.de
Tel.: 0049-89-21804256
Fax: 0049-89-21804176

M. Heuer · K. Bente
Institut für Mineralogie,
Kristallographie und Materialwissenschaft,
Scharnhorststraße 20, 04275 Leipzig, Germany

G. D. Bromiley
Bayerisches Geo-Institut,
Universitätsstr. 30, 95447 Bayreuth, Germany

(CaMgSi₂O₆). Pure CaZnSi₂O₆ is not observed in nature but was synthesized at 900 °C/ 2 GPa by Essene and Peacor (1987). The stability field of end-member petedunnite is restricted to pressures >1 Gpa, as shown experimentally by Rothkopf and Fehr (1998) and Fehr and Huber (2001). First results on the synthesis of hedenbergite–petedunnite solid solutions up to 30 mol% petedunnite at ambient pressures of 0.5 GPa have been reported by Fehr and Hobelsberger (1997).

In nature, hedenbergitic clinopyroxenes and sulfides, such as sphalerite, are common constituents of skarns in phase assemblages with garnet and epidote (e.g. Nakano et al. 1994). An intercrystalline exchange of Fe and Zn occurs between coexisting hedenbergite and sphalerite, resulting in chemical inhomogeneities within the rims of coexisting phases (Fehr and Heuss–Assbichler, 1994). The corresponding intercrystalline exchange reaction can be described by the model reaction:



Zinc contents in hedenbergite coexisting with sphalerite up to 600 and 9000 ppm, respectively, were observed by Nakano et al. (1994) and Fehr and Heuss–Assbichler (1994).

In order to describe the equilibrium conditions and kinetics of the intercrystalline Zn–Fe exchange equilibrium between zincian hedenbergite and ferroan sphalerite, the thermodynamic mixing properties of the solid solution series hedenbergite–petedunnite have to be known. Experimental determinations of thermodynamic mixing properties and diffusion constants require homogeneous material with defined crystal-chemical properties. Therefore, the aim of this study is to synthesize intermediate members of the solid solution series hedenbergite–petedunnite at defined oxygen fugacities and to determine their properties by X-ray diffraction, electron microprobe analysis (EMPA) and ⁵⁷Fe Mössbauer spectroscopy. In addition, clinopyroxene crystals should be suitable for standard single-crystal X-ray structure analysis.

Experimental

Synthesis

Experiments were conducted using pure crystalline phases prepared from sources of reagent grade SiO₂ (99.995%), CaCO₃ (99.999%), Fe₂O₃ (99.99%), Fe (99.999%), FeO (99.9%) and ZnO (99.99%). All oxides, except FeO, were annealed at high temperatures. Three different mixes were prepared by sintering oxides in appropriate portions according to the hedenbergite–petedunnite solid solutions bulk compositions (see Table 1). Oxide mix (I) was prepared by using CaCO₃, Fe, Fe₂O₃ and ZnO, SiO₂ as starting material. Part of the stoichiometric mixtures were annealed at 500 °C 1⁻¹ atm for 36 h (oxide mix Ia), and an aliquot of each was decarbonated at 900 °C 1⁻¹ atm for 36 h (oxide mix Ib). In oxide mix (II) FeO was used as iron source instead of Fe + Fe₂O₃. Appropriate amounts of SiO₂ and CaCO₃ were mixed and decarbonated at 900 °C 1⁻¹ atm for 24 h. ZnO was then added in stoichiometric portions. FeO

was added after the sintering period to prevent oxidation of Fe²⁺. The starting material for oxide mix (III) was a stoichiometric mixture of CaSiO₃ glass, Fe, Fe₂O₃ and SiO₂ (Table 1). During sintering, oxide mix (I) crystallized to quartz, magnetite, haematite, hardystonite, hedenbergite, wollastonite plus calcite (Ia) or zincite (Ib), respectively. Oxide mix (II) crystallized to quartz, magnetite, zincite, larnite and Ca₂Fe₇O₁₁ in various amounts.

All synthesis experiments were conducted in the presence of an oxy-hydrous vapour phase. For oxide mix (Ia), synthesis took place in the presence of a CO₂–H₂O vapour phase, as depicted in Table 1. Hydrous experiments in the temperature range 700 to 900 °C at pressures of 0.2 to 0.7 GPa were conducted using an internally heated gas media apparatus (Yoder 1950; Huckenholz et al. 1975) and a conventional cold-seal pressure vessel (Luth and Tuttle 1963). Temperature and pressure fluctuations were typically ± 5 °C and ± 0.002 GPa. Oxygen fugacity was controlled by the redox condition of the pressure vessel (furnace buffered, $\log f_{\text{O}_2\text{Ni/NiO buffer}} - 0.5$, as proved by H₂ sensor measurements). Experimental methods used here have been described elsewhere (Huckenholz et al. 1974). Starting materials were sealed in platinum capsules with 10 wt% water.

Experiments at higher pressures were performed using a piston-cylinder solid media apparatus. Synthesis of petedunnite was performed in a piston-cylinder solid media apparatus with a low-friction NaCl cell designed by Fehr (1992), exhibiting friction as low as 1%. Temperature and pressure fluctuations were typically ± 5 °C and ± 0.002 GPa, respectively. Some intermediate solid solutions (Hd3g, Hd4g, Hd5g, see Table 1) were synthesized at the Bayerisches Geoinstitut using an end-loaded piston-cylinder type apparatus. Starting mixtures were loaded into 10-mm-long, 5-mm-o.d., 3-mm-i.d. graphite capsules for insertion into the sample assembly. Graphite was chosen for sample encapsulation to control oxygen fugacity during the duration of the experiments. In experiments Hd3g and Hd5g, an additional platinum tube, 6 mm long, 3 mm o.d., 2.8 mm i.d. was placed inside the graphite capsule to separate the sample from the capsule. The platinum tube was open at both ends to allow buffering of the oxygen, but facilitated sample removal after the experiment. In experiment Hd4g, it was necessary to grind the recovered sample and fire the sample at 400 °C/144 h to remove any remaining carbon. The loaded capsules were surrounded by pyrophyllite or Pyrex sample holders and inserted into talc-Pyrex cells with a tapered graphite resistance heater. Pressure was calibrated against the quartz–coesite and kyanite–sillimanite transitions, as well as the melting point of diopside. Temperature was measured with a Pt₉₀Rh₁₀–Pt thermocouple (s type). No correction for the effects of pressure on thermocouple EMF was applied. Experiments were pressurized to 90% of the desired run pressure, heated to the desired temperature, and then further pressurized to the final pressure. Pressure and temperature were monitored and controlled during the duration of the experiments. Experiments were quenched isobarically by shutting off the power whilst maintaining the pressure within ± 0.02 GPa of the run pressure. Quench rates are estimated to be greater than 75 °C s⁻¹. Run conditions for all synthesis experiments are given in Table 1.

After the experiments, the run products were examined by means of oil immersion microscopy, X-ray diffraction and electron microprobe analysis. The electron microprobe (Camebax SX50) was operated at 15 keV acceleration voltage and 15 nA beam current. Synthetic wollastonite (Ca, Si), sphalerite (Zn) and haematite (Fe) were used as standards and matrix correction was performed by PAP procedure (Pouchou and Pichoir 1984). The reproducibility of standard analyses was < 1% for each element routinely analyzed.

X-ray diffraction

For the X-ray diffraction measurements, each sample of the hedenbergite–petedunnite solid solution series was prepared on a low-background sample holder (quartz single-crystal section). The powder diffraction patterns were recorded on a Seifert XRD3003 diffractometer, using a Cu X-ray tube ($\lambda = 1.54056/1.54439 \text{ \AA}$),

Table 1 Experimental conditions and products of synthesis runs

Run	P (GPa)	T (°C)	Buffer ^a	Time (h)	Initial ^b	Results ^c
hed10i	0.2	800	fb	336	Ia	hd (wo, qz, CO ₂ ^v -H ₂ O ^v) ^d
hed10ii	0.2	800	fb	432	Ia	hd (wo, qz, CO ₂ ^v -H ₂ O ^v)
hd10h	1.2	900	–	22	III	hd
hed9i	0.2	700	fb	312	Ia	hd ^{ss} (qz, CO ₂ ^v -H ₂ O ^v)
hed9ii	0.3	800	fb	168	Ia	hd ^{ss} (qz, CO ₂ ^v -H ₂ O ^v)
hed8i	0.2	800	fb	216	Ia	hd ^{ss} (qz, CO ₂ ^v -H ₂ O ^v)
hed8ii	0.3	700	fb	168	Ia	hd ^{ss} (qz, CO ₂ ^v -H ₂ O ^v)
hed7i	0.2	700	fb	168	Ia	hd ^{ss} (qz, CO ₂ ^v -H ₂ O ^v)
hed7ii	0.2	700	fb	168	Ia	hd ^{ss} (qz, CO ₂ ^v -H ₂ O ^v)
hd7b	0.7	720	fb	146.5	Ib	hd ^{ss} (and,qz,wo)
hd5g	1.8	850	C	65	II	hd ^{ss} (and,qz)
hd4g	1.2	990	C	22.5	II	hd ^{ss} (qz)
hd3g	1.8	840	C	64	II	hd ^{ss} (and,qz)
hd2d	2.5	1200	fb	72	II	hd ^{ss} (L)
pd	2.0	1000	fb	69	Ib	pd (L)

^a fb furnace buffer, C graphite capsule

^b Initial oxide mixtures in appropriate portions according to hedenbergite–petedunnite solid solutions bulk compositions: (I) CaCO₃ + Fe + Fe₂O₃ + ZnO + SiO₂ (Ia) annealed at 500 °C, (Ib) annealed at 900 °C, (II) CaO + FeO + ZnO + SiO₂, (III) CaSiO₃(glass) + Fe + Fe₂O₃ + SiO₂

^c hd hedenbergite; hd^{ss} hedenbergite–petedunnite solid solution: pd petedunnite; and andradite; qz quartz, wo wollastonite, L liquid, CO₂^v-H₂O^v: CO₂-H₂O vapour phase

^d Phases in parenthesis traces or less than 5 wt% of total run product

operating at 40 kV and 35 mA. A vertical goniometer in Bragg–Brentano geometry was equipped with a secondary graphite (002)-monochromator to suppress the iron fluorescence radiation and a scintillation detector. Intensity measurements were taken at room temperature in steps of 0.01° over 2θ ranges from 18 to 100 °C with a counting time of 30 s per step. Silicon [*a*₀ = 5.43088(4)Å] or quartz [*a*₀ = 4.91344(4)Å, *c*₀ = 5.40524(8)Å] were used as an internal standard.

Mössbauer spectroscopy

Mössbauer spectra were collected at the Institute of Mineralogy, Salzburg (IMS) and at Department of Earth and Environmental Sciences, Munich (DGU). The spectra were taken using a multi-channel analyzer (IMS: 1024, DGU 512 channels) operating in conjunction with an electromechanical drive system with triangular velocity shape. The velocity range was within ± 4 mm s⁻¹ and the spectrometer velocity was calibrated to the spectrum of sodium nitroprusside. The two simultaneously obtained spectra (IMS: 512 and DGU: 256 channels each) were folded and evaluated assuming Lorentzian line shape. Doublets with equal areas for the low- and high-velocity peaks were used. During the experiments the source (⁵⁷Co/Rh, 50 mCi) and absorber were always kept at room temperature. A duplicate measurement at IMS and DGU displays no significant difference in hyperfine interaction parameters, derived from both spectra. Isomer shifts are reported relative to alpha-iron at room temperature.

Results

Synthesis of hedenbergite–petedunnite solid solution series

Results of synthesis experiments on the hedenbergite–petedunnite solid solution are listed in Table 1. Electron microprobe analyses confirm the stoichiometry of all clinopyroxene syntheses (Table 2). Hedenbergite was synthesized as a single phase over a wide pressure and

temperature range, in agreement with data reported by Turnock et al. (1973). They recommended higher pressures or lower temperatures for the synthesis of hedenbergite to prevent the formation of pyroxenoides such as ferrobustamite. A yield of euhedral hedenbergite crystals up to 70 µm in length and 50 µm in width was observed at higher pressures (1.2 GPa, 900 °C, 22 h, Table 1, Hd10h). Similar-sized hedenbergite crystals were reported by Zhang et al. (1997) from synthesis experiments at 4 GPa and 1150 °C. High-pressure synthesis of hedenbergite was also carried out by Perkins and Vielzeuf (1992), who grew 10–30 µm hedenbergite grains of from high-purity reagents (Fe metal, Fe₂O₃, CaCO₃ and Brazilian quartz) using two cycles. (cycle 1: 1.0 GPa, 1100 °C, 14 h and cycle 2: 1.1 GPa, 1100 °C, 13 h). Haselton et al. (1987) synthesized hedenbergite at 0.9 GPa/1000 °C 6–24 h using a glass starting mix, although their samples had a crystal size of only 1–10 µm. In this study hedenbergite was also synthesized at a lower pressure of 0.2 GPa and at a temperature of 800 °C (Table 1, Hed10i, Hed10ii). Traces of wollastonite and quartz were detected in these runs in addition to hedenbergite with crystal sizes up to 20 µm. Similar results were reported from Gustason (1973), who synthesized hedenbergite crystals up to 20 µm in length from an oxide mixture in a temperature and pressure range of 347 to 912 °C and 0.05 to 2.075 GPa. Below 1 GPa, petedunnite decomposes to willemite–hardystonite–quartz and Zn–feldspar–quartz bearing assemblages at lower pressures (Fehr and Huber 2001). Therefore, synthesis of pure petedunnite was carried out at 2.0 GPa, 1000 °C within 69 h, and produced crystals up to 25 µm. Traces of liquid in the final product suggest that run conditions were close to the liquidus (Table 1, Pd). Essene and Peacor (1987) synthesized petedunnite under

Table 2 Representative electron microprobe analyses of synthetic hedenbergite–petedunnite solid solutions and of natural hedenbergite–diopside solid solutions Fe38. Calculation of chemical formula of clinopyroxene is based on four cations

Run ^a	hed10i	sd ^b	hed10ii	sd ^b	hd10h	sd ^b	hed9j	sd ^b	hed9ii	sd ^b	hed8i	sd ^b	hed8ii	sd ^b	hed7i	sd ^b
SiO ₂	48.09	0.58	49.30	1.47	48.18	0.38	48.44	0.22	48.41	0.27	47.22	1.33	47.37	0.88	48.12	0.37
CaO	21.60	0.71	20.78	0.89	22.95	0.51	22.44	0.35	22.53	0.22	22.42	0.32	22.12	0.71	22.48	0.17
FeO	29.61	0.79	29.99	1.17	29.17	0.68	25.91	0.54	24.42	0.30	21.36	1.34	22.81	0.40	19.15	1.16
ZnO	99.58	0.63	100.06	0.30	100.35	0.60	3.63	0.41	5.16	0.25	8.78	0.98	7.61	0.18	10.68	1.04
Sum							100.42	0.18	100.53	0.39	99.81	0.79	99.91	1.03	100.50	0.50
Si ⁴⁺	2.010	0.016	2.056	0.063	1.983	0.008	2.002	0.003	2.005	0.011	2.018	0.049	1.999	0.012	2.007	0.013
Ca ²⁺	0.967	0.024	0.928	0.037	1.012	0.021	0.993	0.006	1.000	0.009	1.021	0.037	1.001	0.020	1.005	0.009
Fe ²⁺	1.024	0.023	1.016	0.022	0.996	0.024	0.893	0.017	0.837	0.011	0.686	0.044	0.762	0.005	0.660	0.038
Fe ³⁺	0.000	0.000	0.000	0.000	0.008	0.000	0.000	0.000	0.000	0.000	0.000	0.000	0.000	0.000	0.000	0.000
Zn ²⁺							0.111	0.012	0.158	0.007	0.275	0.063	0.238	0.009	0.329	0.042
Run ^a	hed7ii	sd ^b	hed7b	sd ^b	hd5 g	sd ^b	hd4 g	sd ^b	hd3 g	sd ^b	hd2d	sd ^b	pd	sd ^b	Fe38	sd ^b
SiO ₂	47.33	0.35	47.47	0.07	47.51	0.35	47.03	0.37	46.37	0.79	45.98	0.26	47.01	0.36	51.04	0.33
CaO	23.82	0.21	22.49	0.09	21.76	0.30	22.24	0.15	21.65	0.27	21.94	0.21	21.85	0.39	22.87	0.12
FeO	21.44	1.33	18.96	0.25	16.02	1.36	11.70	2.45	7.69	2.76	5.76	0.55			17.75	0.30
ZnO	9.38	1.32	10.81	0.60	15.04	1.29	19.62	2.66	23.76	2.98	26.90	0.82	31.33	0.98		
MgO															6.88	0.12
TiO ₂															0.01	0.02
Al ₂ O ₃															0.36	0.13
MnO															0.79	0.01
Sum	101.96	0.94	99.61	0.37	100.32	0.62	100.59	0.58	99.47	0.49	100.58	0.38	100.26	0.53	99.69	0.39
Si ⁴⁺	2.000	0.009	1.993	0.002	1.994	0.008	1.978	0.008	1.983	0.019	1.953	0.009	2.010	0.012	2.016	0.008
Ca ²⁺	0.971	0.010	1.011	0.005	0.978	0.010	1.002	0.008	0.992	0.014	0.999	0.010	1.001	0.019	0.968	0.007
Fe ²⁺	0.737	0.045	0.662	0.010	0.559	0.048	0.400	0.083	0.266	0.095	0.181	0.017	0.000	0.000	0.586	0.009
Fe ³⁺	0.000	0.000	0.004	0.000	0.003	0.000	0.011	0.002	0.008	0.003	0.023	0.002			0.000	0.000
Zn ²⁺	0.292	0.041	0.331	0.018	0.466	0.040	0.610	0.084	0.751	0.098	0.844	0.026	0.989	0.030		
Mg ²⁺															0.405	0.040
Ti ⁴⁺															0.000	0.000
Al ³⁺															0.003	0.001
Mn ²⁺															0.023	0.003

^a Samples see Table 1

^b Standard deviation (2σ)

similar conditions (2.0 Gpa, 900 °C) over 6 days using glass starting material, although they did not report crystal sizes of the run products.

Intermediate members of the hedenbergite-petedunnite solid solution series were synthesized from oxide mixtures. Experiments were conducted over 22.5 to 312 h in a temperature and pressure range of 700 to 1200 °C and 0.2 to 2.5 GPa, respectively (Table 1). Microprobe analyses suggest that crystals are homogeneous and do not show any chemical zonation (Table 2). Because the starting material contained CaCO₃, Fe-rich solid solution up to 0.3 Zn pfu was synthesized at pressures up to 0.7 GPa in the presence of a binary H₂O–CO₂ vapour phase (with exception of run Hd7b, which was conducted under hydrous conditions). Zn-rich solid solutions with compositions between 0.46 < Zn pfu < 0.84 were synthesized at pressures up to 2.5 GPa. Traces of liquid in the run product suggest that the sample with the highest Zn content (Table 1, Hd2), was synthesized close to the liquidus. The crystal sizes of intermediate members of hedenbergite–petedunnite solid solutions vary from 20 to 80 µm.

XRD and determination of the unit-cell parameters

Phase analyses by X-ray diffraction show that the main components in all samples were clinopyroxenes. Traces of quartz, andradite and wollastonite were noted in some run products (Table 1). Sharp reflections with small half-widths indicate a good sample crystallinity and quality.

Rietveld analysis was performed simultaneously for both sample and internal standard using the program WYRIET3 (Schneider and Young 1993). Correction parameters (zero shift, sample displacement) were initially refined, with fixed unit-cell parameters for the internal standard. Unit-cell parameters for the solid solution member were then refined. The refinements converged at R_P values of 8–10% and R_{WP} values of 11–14%. The R_{Bragg} referring to the clinopyroxene phase

reached values of 6–8%. Constraints on chemistry and site occupancy were based on the results of the microprobe analysis (Table 2) with the assumption that Fe²⁺ and Zn²⁺ share the M1 site and that Ca²⁺ fully occupies the M2 site. Preferred orientations in (310) and (150) were corrected by a March–Dollase function. Calculations were based on the structure model of a clinopyroxene by Cameron et al. (1973). Due to the high overlap of reflections, the Rietveld method provides a more accurate determination of lattice parameters than conventional fitting of reflections with single profiles. The calculations were carried out starting with a structure model of a clinopyroxene by Cameron et al. (1973). In this study the Rietveld method was used only for the determination of unit-cell parameters and not for the refinement of any other structural data such as atomic coordinates and site occupancies. Rietveld refinements of these parameters were not meaningful because of high parameter correlations and the low scattering contrast between Zn and Fe. Refinements on single-crystal data of hedenbergite–petedunnite solid solution are necessary in order to obtain significant results (Heuer et al. 2002a,b).

The unit-cell parameters of the synthetic samples are listed in Table 3 and shown in Fig. 1a. Values of the unit-cell parameters for pure hedenbergite are similar to data found for an Fe³⁺-free sample characterized by Redhammer et al. (2000). The unit-cell parameters of pure petedunnite corresponds with values reported for synthetic CaZnSi₂O₆ by Essene and Peacor (1987), although they report large errors in their value (Table 3). Figure 1a shows the variation in lattice parameters as a function of petedunnite component. Parameters a_0 and b_0 exhibit a linear decrease with increasing Zn content while the monoclinic angle β increases linearly. Parameter c_0 is not affected by composition and remains constant at an average value of 5.248 Å. The presence of a minor amount of a Ca–ferri–Tschermak's component (Ca–Fe³⁺–Fe³⁺–SiO₆) in Zn-rich samples Hd4g and Hd2b, as shown by Mössbauer spectroscopy (see below), does not significantly affect the unit-cell parameter. Cell volume

Table 3 Values of the refined unit-cell parameters. Numbers in parentheses denote standard deviation (2σ). Fe²⁺ pfu Ferrous iron per formula unit, based on microprobe and Mössbauer analyses

Sample	Fe ²⁺ (pfu)	a_0 (Å)	b_0 (Å)	c_0 (Å)	β (deg)	Cell vol (Å ³)	> Molar vol (cm ³)
hed10ii	1	9.8455(12)	9.0225(8)	5.2511(4)	104.82(1)	450.94(90)	33.94(8)
Hd10 h	1	9.8462(6)	9.0271(6)	5.2575(4)	104.77(1)	450.99(90)	33.95(8)
hed9i	0.89	9.8413(8)	9.0210(8)	5.2507(4)	104.97(1)	450.32(90)	33.89(8)
hed8i	0.69	9.8351(6)	9.0111(3)	5.2544(3)	105.09(1)	449.62(90)	33.84(8)
hed8ii	0.76	9.8385(6)	9.0166(6)	5.2523(3)	105.06(1)	449.93(90)	33.87(8)
hed7i	0.66	9.8330(8)	9.0108(8)	5.2514(4)	105.14(1)	449.14(90)	33.81(8)
hed7ii	0.74	9.8347(6)	9.0119(6)	5.2535(3)	105.15(1)	449.43(90)	33.83(8)
hd5g	0.56	9.8206(8)	8.9966(8)	5.2487(4)	105.34(1)	447.21(90)	33.66(8)
hd4g	0.40	9.8150(6)	8.9921(6)	5.2499(3)	105.50(1)	446.49(90)	33.61(8)
hd3g	0.27	9.8068(7)	8.9818(8)	5.2484(7)	105.62(1)	445.22(90)	33.51(8)
hd2d	0.18	9.8093(7)	8.9817(7)	5.2527(4)	105.66(1)	445.63(90)	33.54(8)
pd	0	9.7989(6)	8.9792(6)	5.2490(4)	105.98(1)	443.99(90)	33.42(8)
pd ^a	0	9.803(6)	8.975(7)	5.243(7)	105.75(7)	444(2)	33.4(2)

^a Synthetic petedunnite from Essene and Peacor (1987)

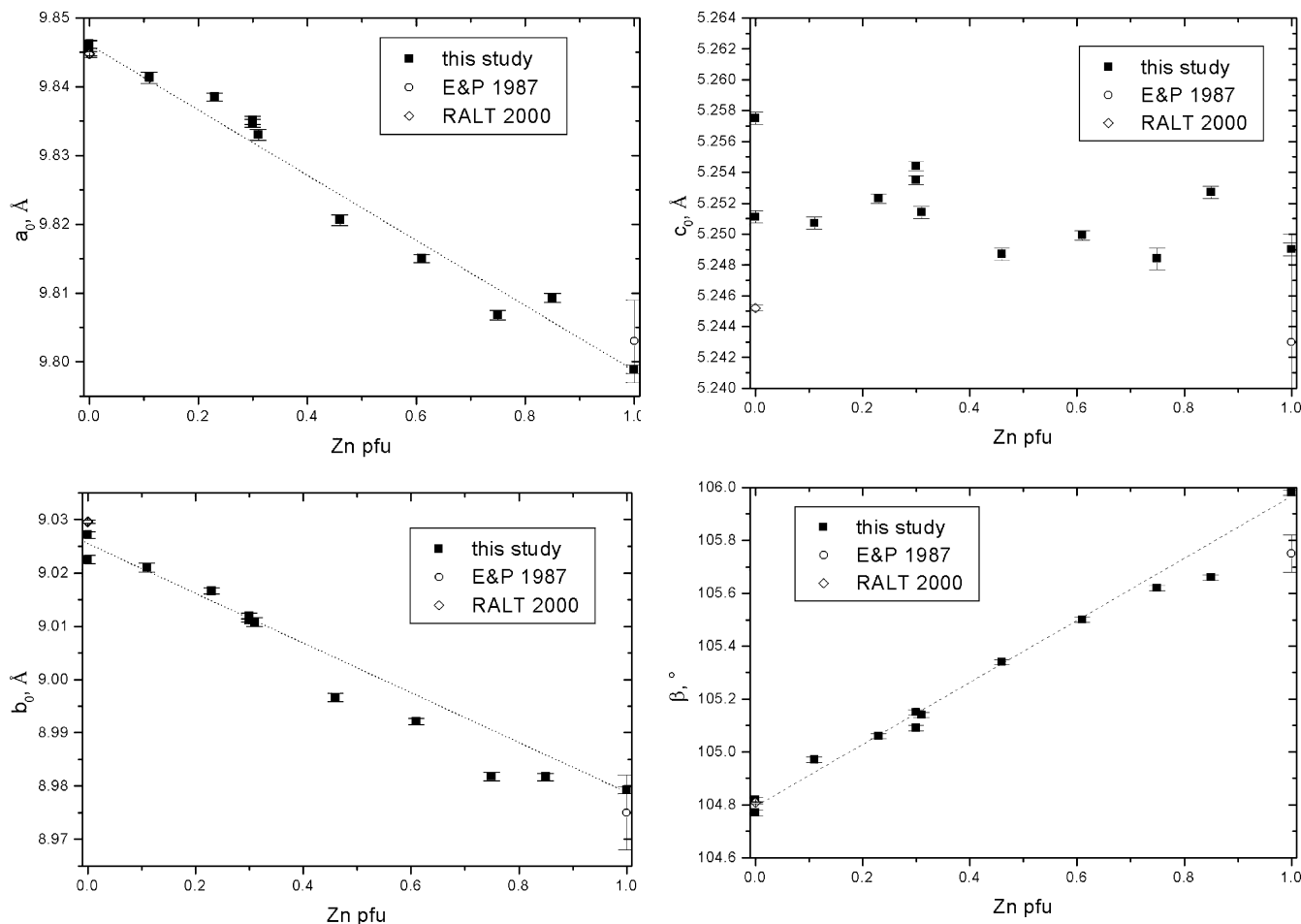


Fig. 1 a Unit-cell parameter along the join hedenbergite–pettedunnite. Data are given in Table 3. *E&P 1987* Essene and Peacor (1987); *RALT 2000* Redhammer et al. (2000)

and molar volume also decrease linearly with increasing pettedunnite component as shown in Fig. 1b. The effect of changing molar volume with composition can be described by the equation V_{mol} (ccm mol^{-1}) = $33.963(16) - 0.544(31) \cdot \text{Zn pfu}$ with a regression coefficient of $r^2 = 0.969$, indicating the absence of excess mixing molar volume along the join hedenbergite–pettedunnite.

Mössbauer spectroscopy

^{57}Fe Mössbauer spectroscopy was used to determine the valence state and site occupancy of iron and to check the quality of synthesized clinopyroxenes. The ^{57}Fe hyperfine parameters of intermediate samples along the hedenbergite–pettedunnite join are listed in Table 4 and fitted spectra of selected specimen are shown in Figs. 2 to 5. In hedenbergite, Fe is restricted to the M1 site, and in the Mössbauer spectrum only one doublet of ferrous iron occurs (Fig. 2). The spectrum displays a small asymmetry at a higher intensity on the high-velocity side, which was reported also by Tennant et al. (2000).

The isomer shift of $1.18\text{--}1.19 \text{ mm s}^{-1}$ and quadrupole splitting of $2.24\text{--}2.26 \text{ mm s}^{-1}$ are characteristic for Fe^{2+} on an octahedral site. Similar parameters were reported for hedenbergite by Redhammer et al. (2000), who synthesized samples at lower oxygen fugacities using magnetite–wuestite and iron–quartz–fayalite buffers, as shown in Figs. 6 and 7. The small half-widths of 0.27 to 0.29 mm s^{-1} show that we studied a homogenous and well-crystallized sample in agreement with the X-ray powder diffraction pattern. Neither Fe^{2+} on the eight-fold-coordinated M2 site nor tetrahedral Fe^{3+} was detected in accordance with the microprobe analyses (see Table 2). The Mössbauer parameters are in accordance with results for Fe^{2+} on octahedral sites in other minerals such as epidotes (Dollase 1973; Lipka et al. 1995; Fehr and Heuss–Assbichler 1997) or Ti-andradite (Kühberger et al. 1989). The spectra for intermediate solid solutions show one doublet of ferrous iron only and display no asymmetry, as illustrated in Fig. 3. The significance of the signals resulting from Zn-containing hedenbergite was lower, because of Zn absorption, resulting in higher backgrounds. Some intermediate samples (Hd7b, Hd5g, Hd3g) exhibit an additional doublet, as shown in Fig. 4. The isomer shift of $0.38\text{--}0.44 \text{ mm s}^{-1}$ and quadrupole splitting of $0.61\text{--}0.70 \text{ mm s}^{-1}$ are characteristic for Fe^{3+} on octahedral

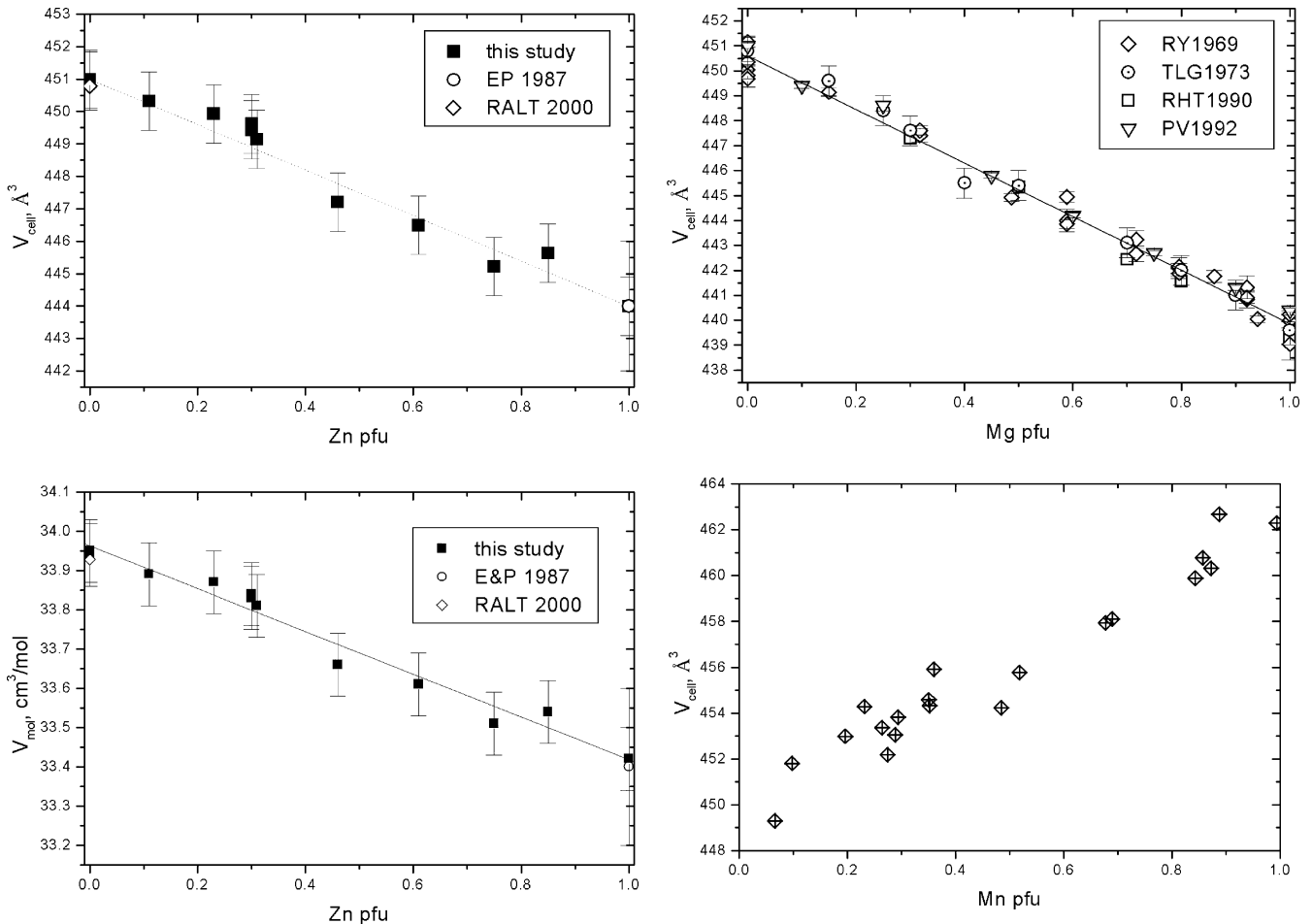


Fig. 1 b Cell volume and molar volume along the join hedenbergite–pettedunnite. Data are given in Table 3. *E&P 1987* Essene and Peacor (1987); *RALT 2000* Redhammer et al. (2000)

Fig. 1 c Cell volume along the join hedenbergite–diopside (*RY1969* Rutstein and Yund, 1969; *TLG1973* Turnock et al. 1973; *RHT1990* Raudsepp et al. 1990; *PV1992* Perkins and Vielzeuf 1992) and hedenbergite–johannesite (Capitani and Mellini 2000)

site. These three intermediate samples are not single-phase clinopyroxenes but contain andradite as a minor phase (Table 1). The Mössbauer parameters of the second doublet are close to the one found for andradite ($\delta = 0.40 \text{ mm s}^{-1}$, $\Delta E_Q = 0.56 \text{ mm s}^{-1}$; Armbruster and Geiger 1993) and therefore can be attributed to ferric iron on octahedral site in andradite. Microprobe analyses for these three clinopyroxene samples show no charge balance deficiencies (Table 2), indicating the absence of ferric iron. The Mössbauer spectra of two intermediate solid solutions (Hd4g and Hd2d, see Table 4) consist of three doublets, as shown in Fig. 5. The isomer shifts of 1.18 mm s^{-1} and the quadrupole splittings of 1.99 and 2.11 mm s^{-1} of the most intense doublet are characteristic for Fe^{2+} on the octahedral site (see Table 4). The isomer shift of 0.22 – 0.27 mm s^{-1} of the other two doublets is characteristic for ferric iron. The synthesis products do not contain andradite or any other ferric-iron-bearing phase (see Table 1), indicating that the ferric iron is incorporated in the clinopyroxene. The quadrupole splitting of 0.92 – 1.00 mm s^{-1} of one doublet is similar to data for Fe^{3+} on the octahedral site

in esseneite ($\text{CaAl}^{3+}\text{Fe}^{3+}\text{SiO}_6$) (0.99 mm s^{-1} ; Akasaka 1983), natural diopside–esseneite solid solution (0.96 mm s^{-1} ; De Grave et al. 2002) or diopside–Ca–ferri–Tschermak’s molecule ($\text{CaFe}^{3+}\text{Fe}^{3+}\text{SiO}_6$) solid solution (1.01 – 1.07 mm s^{-1} ; Hafner and Huckenholz 1971), but differ significantly from quadrupole splitting of 0.28 – 0.33 mm s^{-1} for ferric iron on the octahedral site in pure aegirine (Redhammer et al. 2000). The quadrupole splitting of 1.38 – 1.49 mm s^{-1} of the other doublet is similar to that found for Fe^{3+} on the tetrahedral site in esseneite (1.58 mm s^{-1} ; Akasaka 1983), natural diopside–esseneite solid solution (1.38 mm s^{-1} ; de Grave et al. 2002) or diopside–Ca–ferri–Tschermak’s molecule solid solution (1.49 – 1.62 mm s^{-1} ; Hafner and Huckenholz 1971, 1.48 – 1.56 mm s^{-1} ; Redhammer 1998). The intensities of ferric iron on octahedral and tetrahedral sites are equal, indicating the presence of a ferri–Tschermak’s component of 3.5 ± 1 and $3.2 \pm 1 \text{ mol}\%$ in samples Hd4g and Hd2d, respectively. The Mössbauer spectrum of a natural hedenbergite–diopside solid solution was taken for comparison, and consists of only one doublet. The isomer shift of 1.19 mm s^{-1} and

Table 4 ^{57}Fe Mössbauer parameters for Fe^{2+} on M1 and Fe^{3+} in clinopyroxenes at room temperature. Fe^{2+} pfu Ferrous iron per formula unit, based on microprobe and Mössbauer analyses; δ isomer shift relative to alpha iron at 295 K (± 0.01 m ms^{-1}); ΔE_Q :

Sample	Fe^{2+} (pfu)	δ (mm s^{-1})	$\text{Fe}^{2+} \Delta E_Q$ (mm s^{-1})	Γ (mm s^{-1})	Area (%)	δ (mm s^{-1})	$\text{Fe}^{3+} \Delta E_Q$ (mm s^{-1})	Γ (mm s^{-1})	Area (%)	χ^2
hed10i	1	1.18	2.24	0.27	100.0				0.0	1.14
hd10h	1	1.19	2.26	0.29	100.0				0.0	0.96
hed9ii	0.84	1.17	2.20	0.26	100.0				0.0	0.34
hed8ii	0.76	1.18	2.22	0.26	100.0				0.0	0.38
hd7b	0.66	1.18	2.15	0.28	89.4	0.44	0.70	0.22	10.6	0.83
hd5g	0.56	1.19	2.10	0.38	96.2	0.38	0.70	0.20	3.8	0.90
hd4g	0.40	1.18	2.11	0.31	93.0	0.27	1.00	0.22	3.6	0.50
						0.22	1.49	0.35	3.5	
hd3g	0.27	1.19	2.01	0.33	97.8	0.40	0.61	0.22	2.2	0.50
hd2d	0.18	1.18	1.99	0.29	93.5	0.22	0.92	0.22	3.3	0.48
						0.23	1.38	0.23	3.2	
Fe38	0.59	1.19	2.11	0.32	100.0				0.0	0.91

quadrupole shift (± 0.01 m ms^{-1}); Γ full line width at half peak height (± 0.01 mm s^{-1}); *area* area referred to the full absorption area = 100% ($\pm 1\%$), χ^2 per channel

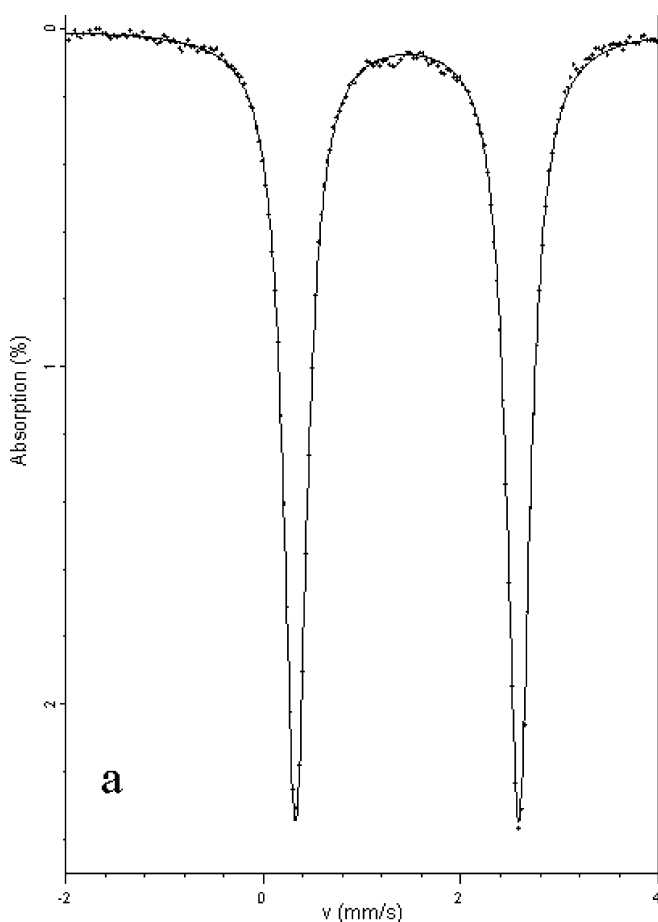


Fig. 2 Mössbauer spectrum of hedenbergite hed10i taken at 295 K absorber temperature. The spectrum has been evaluated by one doublet

quadrupole splitting of 2.11 mm s^{-1} are characteristic for Fe^{2+} on octahedral site (Fe38 in Table 4) and are close to that found for a hedenbergite–petedunnite solid solution of similar iron content (Hd5 g in Table 4). The isomer shifts of ferrous iron on the M1 site in heden-

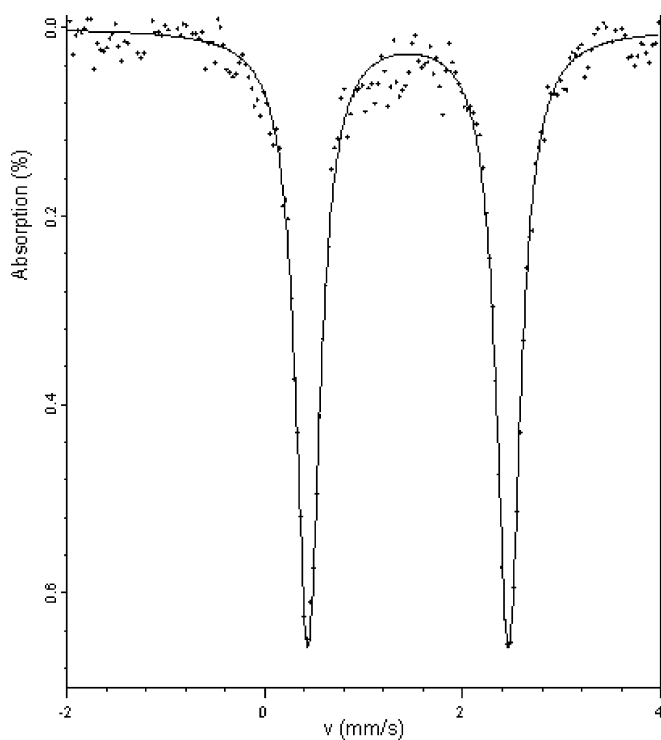


Fig. 3 Mössbauer spectrum of hedenbergite–petedunnite solid solution hed8ii (0.783 Fe pfu) taken at 295 K absorber temperature. The spectrum has been evaluated by one doublet

bergite are not affected by the changing composition. With increasing Zn content they remain constant at an average value of 1.18 mm s^{-1} , as shown in Table 4 and Fig. 6. In turn, the quadrupole splittings of Fe^{2+} on M1 are strongly affected by the composition of intermediate solid solution. They decrease linearly with increasing petedunnite component in hedenbergite, ranging from 2.25 mm s^{-1} of pure hedenbergite end member to 1.99 mm s^{-1} of a solid solution containing 84 mol% petedunnite (Hd2d in Table 4). With the exception of sample Hd5 g, which displays a half-width of

0.38 mm s⁻¹, all the half-widths of intermediate solid solution vary between 0.26 and 0.33 mm s⁻¹ and are comparable to 0.32 mm s⁻¹ found for the natural hedenbergite–diopside solid solution Fe38 (see Table 4).

Figure 8 clearly illustrates that the half-widths are not affected by composition, pressure, temperature or by the type of initial material.

Discussion

Clinopyroxenes along the join hedenbergite–petedunnite can be synthesized as pure single-phase products under hydrothermal conditions in the presence of an oxy-hydrous vapour phase from highly unstable initial oxide mixtures. Crystal sizes up to 70 μm of intermediate members can be suitable for standard single-crystal X-ray analysis (Heuer et al. 2002a,b). In turn, tiny crystal sizes < 8 μm were observed in synthesis products of hedenbergite composition using gel (Nolan 1969; Kinrade et al. 1975; Kawasaki and Ito 1994; Redhammer et al. 2000) or ferrobustamite (Moecher and Chou 1990) as initial material. X-ray diffraction, Mössbauer spectra and microprobe analysis demonstrate that all members of the hedenbergite–petedunnite solid solution are well crystallized. During synthesis, the growth kinetics of the run products are mainly controlled by reaction time, as shown in Fig. 8. After 180 h curing time, clinopyroxenes of various compositions and synthesis conditions exhibit a minimum line width of 0.26 mm s⁻¹, considerably smaller than that of pure hedenbergite (Γ = 0.32 mm s⁻¹), synthesized from gels for 1369 h (Redhammer et al. 2000). Kinrade et al. (1975) studied the crystallization kinetics of hedenbergite from gels by means of Mössbauer spectroscopy. They reported that the formation of hedenbergite was

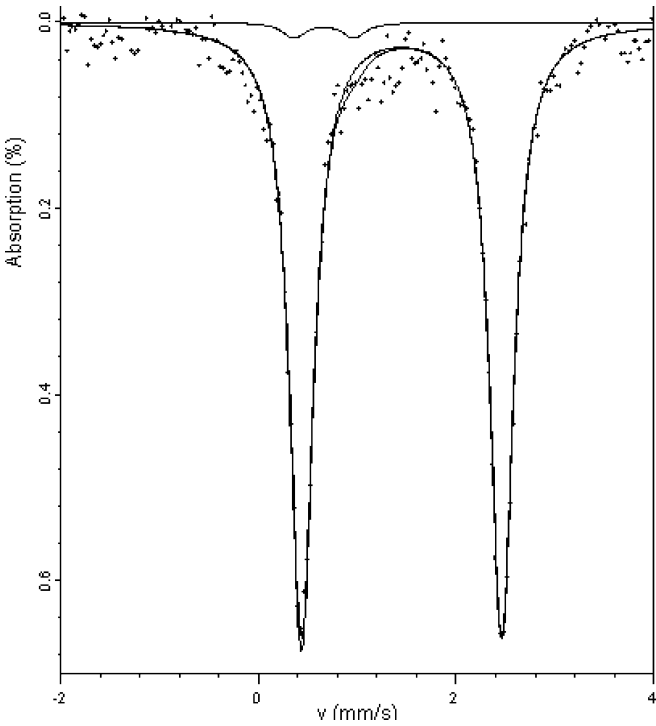


Fig. 4 Mössbauer spectrum of hedenbergite–petedunnite solid solution hd3g (0.230 Fe pfu) taken at 295 K absorber temperature. The spectrum has been evaluated by two doublets

Fig. 5 Mössbauer spectrum of hedenbergite–petedunnite solid solution hd4g (0.390 Fe pfu) taken at 295 K absorber temperature. The spectrum has been evaluated by three doublets

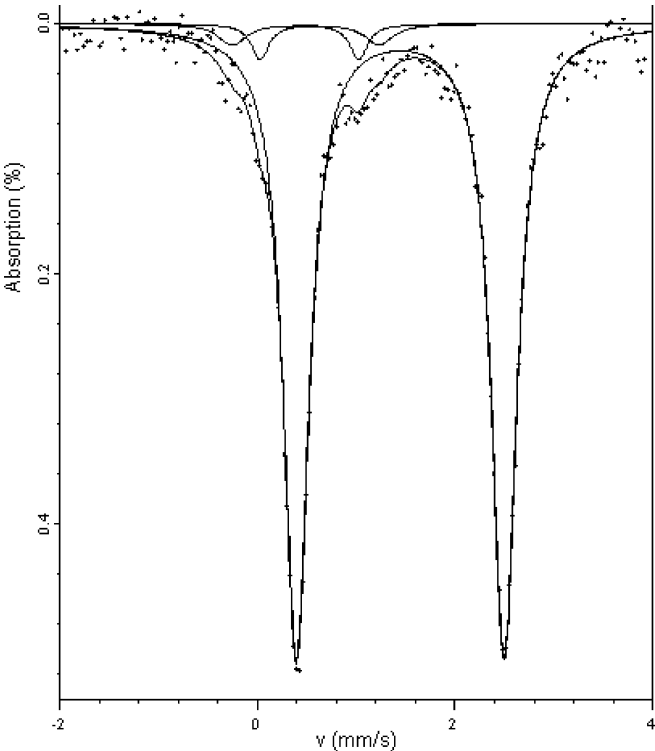


Fig. 6 Isomer shift of ferrous iron on octahedral site at room temperature of natural and synthetic hedenbergite solid solutions as function of hedenbergite component. Data are relative to alpha-iron and are given in Table 4. Abbreviations are *DG 1982* Dollase and Gustafson (1982); *RALT 2000* Redhammer et al. (2000); *BWB 1971* Bancroft et al. (1971); *A&R 1984* Amthauer and Rossman (1984); *TMM 2000* Tennant et al. (2000)

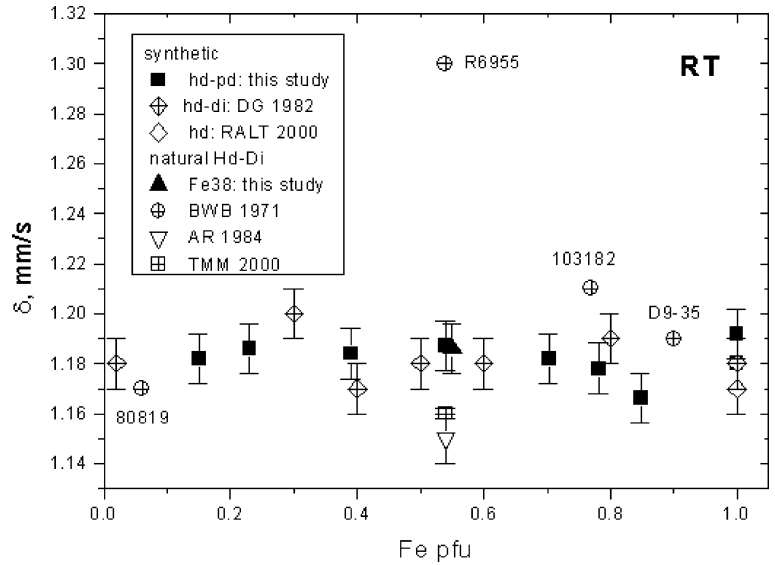


Fig. 7 Quadrupole splitting of ferrous iron on octahedral site at room temperature of natural and synthetic hedenbergite solid solution as function of hedenbergite component. Data are given in Table 4. Abbreviations are *DG 1982* Dollase and Gustafson (1982); *RALT 2000* Redhammer et al. (2000); *BWB 1971* Bancroft et al. (1971); *A&R 1984* Amthauer and Rossman (1984); *TMM 2000* Tennant et al. (2000)

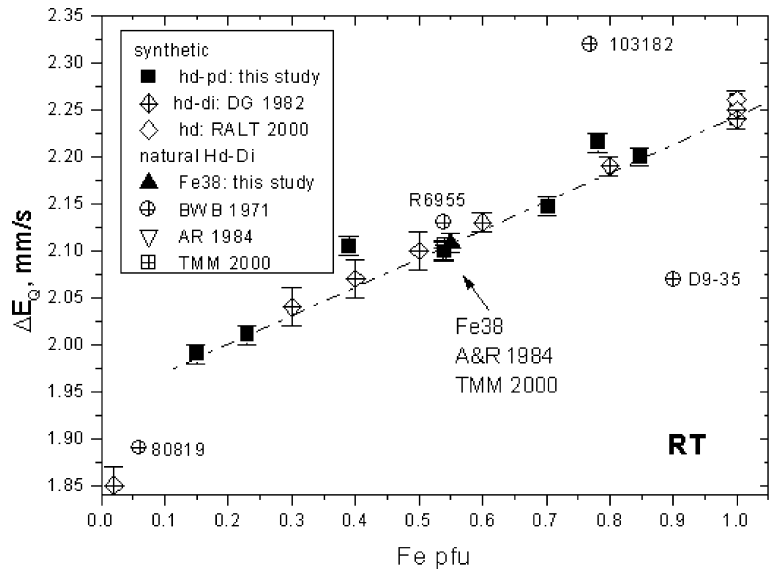
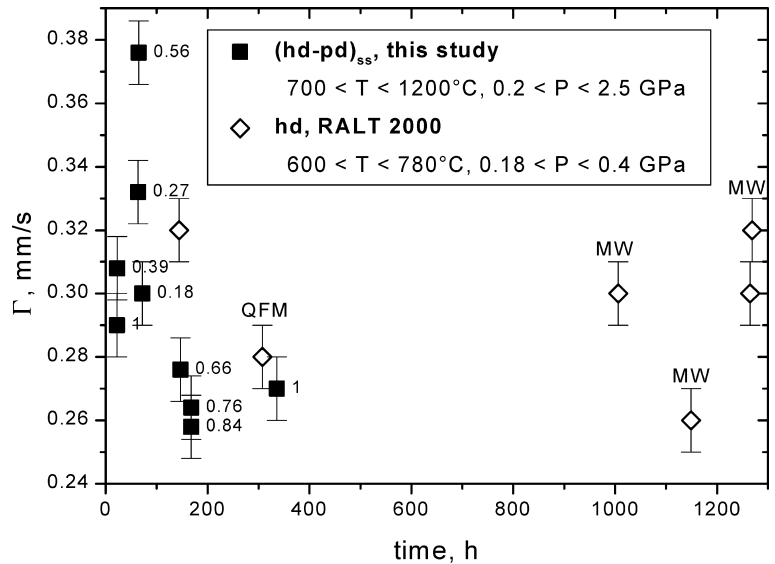


Fig. 8 Line width of ferrous iron on octahedral site at room temperature of petedunnite–hedenbergite solid solutions as function of synthesis time. Data are given in Table 4. Numbers denote Fe^{2+} pfu. Abbreviations are *QFM* quartz–fayalite–magnetite solid-state oxygen buffer; *MW* magnetite–wuestite solid-state oxygen buffer; *RALT 2000* Redhammer et al. (2000), pure hedenbergite end member

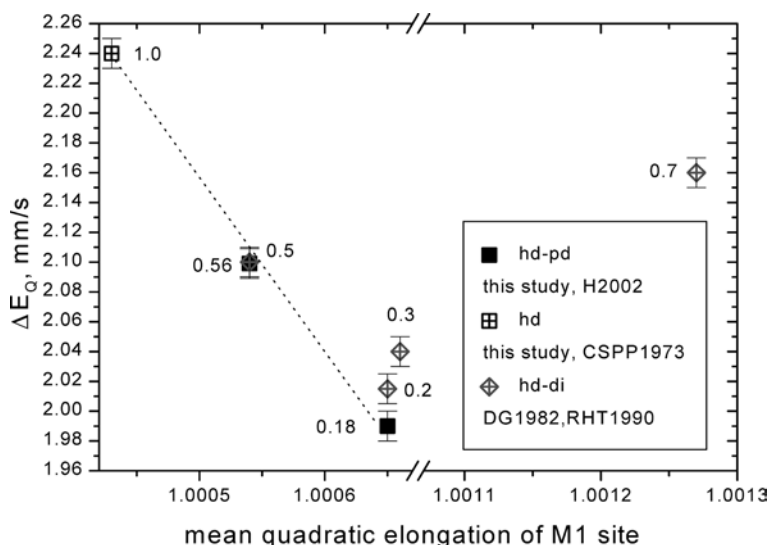


essentially complete after 2.5 h at 450 °C, 0.1 GPa. Unfortunately, they gave no Mössbauer parameter to prove the crystallinity of their synthesis products. The data of this study clearly demonstrate that the crystallinity of hedenbergitic clinopyroxenes can be improved by using oxide mixtures as starting material. The use of oxide mixtures as initial material also avoids the occurrence of ferrobustamite at high iron contents, as observed in crystallizing gels along the join hedenbergite–diopside (Raudsepp et al. 1990).

The crystal chemistry of hedenbergite–petedunnite solid solution exhibits some similarities with hedenbergite–diopside solid solution, despite the slightly different effective ionic radii of Zn (0.74 Å) and Mg (0.72 Å) (Shannon 1976). The isomer shifts of synthetic and natural members of both solid solutions are not affected by composition (Fig. 6). The character of the chemical bonding of Fe^{2+} does not change by substituting Mg or Zn onto the octahedral M1 site, as indicated by a constant isomer shift of 1.18 mm s⁻¹. Based on Mössbauer studies, a similar behaviour is also reported for the substitution of Fe^{2+} by trivalent cations like Fe^{3+} or Cr^{3+} in hedenbergitic clinopyroxenes (Dollase and Gustafson 1982; Redhammer et al. 2000). In turn, the quadrupole splitting of ferrous iron on the M1 site are strongly affected by composition along the binary joins hedenbergite–petedunnite and hedenbergite–diopside (Fig. 7). The quadrupole splittings of Fe^{2+} decrease linearly with decreasing hedenbergite component at the same rate, independently of the substituting cation, implying the same distortion of the nuclear electric field gradient. The electric field gradient is controlled by a lattice term and a valence term (Dowty and Lindsley 1973, Dollase and Gustafson 1982). The first effect is produced by deviation of the cubic symmetry in the atomic arrangement surrounding an iron atom, and the second effect can be attributed to deviation from the cubic symmetry of the six *d* electrons of Fe^{2+} itself. The Fe^{2+} doublets in the clinopyroxenes studied show a

variation of 0.3 mm s⁻¹ across the binary joins up to a composition of 0.1 Fe pfu (Bancroft et al. 1971; Dollase and Gustafson 1982; Amthauer and Rossman 1984; Tennant et al. 2000; this study), followed by a rapid decrease of quadrupole splitting to more iron-poor compositions, as illustrated in Fig. 7. According to Dollase and Gustafson (1982), this variation can be attributed to the compositional variation of the lattice term. On the other hand, Dowty and Lindsley (1973) stated in their model for Ca–Na–clinopyroxenes that significantly different valence terms were possible due to changes in occupancy of the surrounding M2 site, resulting in a change of orbital configuration. In hedenbergite–petedunnite and hedenbergite–diopside solid solutions, the M2 site is occupied by Ca and the orbital configuration of Fe^{2+} on M1 site should stay constant across both the binary joins. The distortion of an octahedral site can be expressed by its mean quadratic elongation (Robinson et al. 1971). Based on single-crystal structure refinement, end-member hedenbergite exhibits a less distorted M1 site, characterized by a mean quadratic elongation of 1.00012 and a quadrupole splitting of 2.24 mm s⁻¹ (this study), as shown in Fig. 9. It was found for intermediate hedenbergite–petedunnite solid solution by single-crystal refinements, that the M1–O lengths lying in the *a*–*b* plane, are shorter than in pure hedenbergite, but there are no changes for the M1–O lengths along the *c* direction (Heuer et al. 2002a,b). Based on these data, a mean quadratic elongation of 1.00054 and 1.00065 can be calculated for a composition 0.56 Fe^{2+} pfu and 0.18 Fe^{2+} pfu, respectively. Figure 9 illustrates that increasing distortion of the M1 site occurs with decreasing hedenbergite component. Mean quadratic elongations of intermediate members of hedenbergite–diopside solid solution, based on Rietveld refinements of powder samples by Raudsepp et al. (1990) and of Mössbauer data by Dollase and Gustafson (1982), are also shown in Fig. 9. If sample Hd₇₀Di₃₀ is disregarded, clinopyroxenes of both solid solution series

Fig. 9 Quadrupole splitting of ferrous iron on octahedral M1 site at room temperature of synthetic hedenbergite solid solutions as function of mean quadratic elongation. Data for hedenbergite–petedunnite are given in Table 4. Numbers denote Fe^{2+} pfu. Abbreviations are *hd* hedenbergite; *pd* petedunnite; *di* diopside; *H2002* Heuer et al. (2002a,b); *CSPP1973* Cameron et al. (1973); *DG 1982* Dollase and Gustafson (1982); *RHT 2000* Raudsepp et al. (1990)



follow the same linear trend: quadrupole splittings of Fe^{2+} decrease with increasing distortion of M1 site, indicating that the electric nuclear field gradient is mainly controlled by the lattice term. Additional effects probably only occur in iron-poor compositions (<0.1 Fe pfu), as indicated by the rapid decrease of quadrupole splitting (Fig. 7). Molecular orbital calculations for epidotes (Grodzicki et al. 2001) have shown that the quadrupole splitting is affected not only by the next neighbours surrounding an iron atom, but also by the second and third coordination shell of a site.

Despite distortion of the M1 site, a linear dependence of composition is also documented in the molar volume along the join hedenbergite–petedunnite (Fig. 1b). A similar behaviour in accordance with Vegard law is also reported for the binary joins hedenbergite–diopside (Rutstein and Yund 1969; Turnock et al. 1973; Raudsepp et al. 1990; Perkins and Vielzeuf 1992) and hedenbergite–johannsenite (Capitani and Mellini 2000; Fig. 1c). The molar volumes clearly demonstrate that no excess volume exists in hedenbergitic clinopyroxenes concerning the errors of data. In turn, the thermodynamic mixing behaviour is non-ideal along the hedenbergite–diopside join and mixing properties have to be described by an asymmetric Margules equation (Davidson 1985; Davidson and Lindsley 1985; Sack and Ghiorso 1994).

Despite large errors in the molar volume data, Kawasaki and Ito (1994) developed a thermodynamic mixing model using excess function for the mixing volume. Preliminary results on the mixing properties along the join hedenbergite–petedunnite imply a non-ideal asymmetric behaviour (Fehr and Hobelsberger 1997; Huber and Fehr 2002). The absence of excess molar volumes in both solid solution series indicates that the activity coefficients of each component do not depend on pressure, but on composition and temperature.

Conclusions

Members of the solid solution series hedenbergite–petedunnite $\text{Ca}(\text{Fe,Zn})\text{Si}_2\text{O}_6$ were synthesized under hydrothermal conditions and different oxygen fugacities at temperatures of 700 to 1200 °C and pressures of 0.2 to 2.5 GPa. The small half-widths of ^{57}Fe Mössbauer spectra, X-ray diffraction pattern and microprobe examination show that homogeneous and well-crystallized samples were synthesized. Molar volume across the join hedenbergite–petedunnite varies linearly with composition and does not exhibit an excess molar volume, as in other hedenbergitic clinopyroxenes. The character of chemical bonding does not change by substituting Zn in hedenbergite, as demonstrated by a constant isomer shift of 1.18 mm s^{-1} , and the same behaviour is observed for the replacement of Fe^{2+} by Mg. In turn, the quadrupole splittings across the join hedenbergite–petedunnite do not remain constant but decrease with decreasing Fe content, as

observed in the hedenbergite–diopside solid solution. This variation of the nuclear electric field gradient can be attributed to an increasing distortion of the M1 site, as the distortion increases with increasing petedunnite or diopside component, respectively. The distortion on the M1 site obviously affects the thermodynamic mixing properties of the hedenbergite–petedunnite solid solution and leads to a non-ideal behaviour. The absence of an excess mixing volume indicates that the activity coefficients are independent of pressure.

Acknowledgements The authors thank Prof. G. Amthauer, Salzburg, for use of the Mössbauer spectroscopy equipment, Prof. L. Cemic and P. Kluge, Kiel and Dr. G. Redhammer, Aachen, for high-pressure synthesis of hedenbergite samples and H. Lohringer for preparing microprobe samples. We thank the Deutsche Forschungsgemeinschaft (DFG) for granting the project under Fe235/5 and Be1088/11 in the priority program Experimentelle Studien über Elementverteilung.

References

- Akasaka M (1983) ^{57}Fe Mössbauer study of clinopyroxenes in the join $\text{CaAl}^{3+}\text{Fe}^{3+}\text{SiO}_6$ – $\text{CaTiAl}_2\text{O}_6$ *Phys Chem Miner* 9: 205–211
- Amthauer G, Rossman GR (1984) Mixed valence of iron in minerals with cation clusters. *Phys Chem Miner* 11: 37–51
- Armbruster T, Geiger C (1993) Andradite crystal chemistry, dynamic X-site disorder and the structural strain in silicate garnets. *Eur J Miner* 5:59–72
- Bancroft GM, Williams PGL, Burns RG (1971) Mössbauer spectra of minerals along the diopside–hedenbergite tie line. *Am Mineral* 56: 1617–1625
- Burton JC, Taylor LA, Chou I-M (1982) The f_{O_2} – T and f_{S_2} – T stability relations of hedenbergite and of hedenbergite–johannsenite solid solutions. *Econ Geol* 77: 764–783
- Cameron M, Sueno S, Prewitt CT, Papike JJ, (1973) High-temperature crystal chemistry of acmite, diopside, hedenbergite, jadeite, spodumene, and ureyite. *Am Mineral* 58: 594–618
- Capitani GC, Mellini M (2000) The johannsenite-hedenbergite complete solid solution: clinopyroxenes from the Campiglia Marittima skarn. *Eur J Miner* 12: 1215–1227
- Clark JR, Appleman DE, Papike JJ (1969) Crystal-chemical characterization of clinopyroxenes based on eight new structure refinements. *Mineral Soc Am, Spec Pap* 2: 31–50
- Davidson PM (1985) Thermodynamic analysis of quadrilateral pyroxenes. I Derivation of the ternary non-convergent site-disorder model. *Contrib Mineral Petrol* 91: 383–389
- Davidson PM, Lindsley DH (1985) Thermodynamic analysis of quadrilateral pyroxenes. II Model calibration from experiments and applications to geothermometry. *Contrib Mineral Petrol* 91: 390–404
- de Grave J, de Paep P, de Grave E, Vochten R, Eeckhout SG (2002) Mineralogical and Mössbauer spectroscopic study of a diopside occurring in the marbles of Andranondambo, Madagascar. *Am Mineral* 87: 132–141
- Dollase WA (1973) Mössbauer spectra and iron distribution in the epidote-group minerals. *Z. Kristallogr* 138: 41–63
- Dollase WA, Gustafson WI (1982) ^{57}Fe Mössbauer spectral analysis of sodic clinopyroxenes. *Am Mineral* 67: 311–327
- Dowty E, Lindsley DH (1973) Mössbauer spectra of synthetic hedenbergite–ferrosilite pyroxenes. *Am Mineral* 58: 850–868
- Essene EJ, Peacor DR (1987) Petedunnite ($\text{CaZnSi}_2\text{O}_6$), a new zincian clinopyroxene from Franklin, New Jersey, and phase equilibria for zincian pyroxenes. *Am Mineral* 72: 157–166
- Fehr KT (1992) Petrogenetische Teilnetze für Niedertemperatur-Hochdruck (LT-HP) Metamorphite im System Ca – Al – Fe^{3+} – Ti – Si – O – H . Habilitation Thesis University Munich 211p

- Fehr KT, Heuss-Assbichler S (1994) The trace-element content of Zn in garnet, clinopyroxene and epidote as a petrogenetic indicator. *Terra Abstr* No.1, *Terra Nova* 6: 23
- Fehr KT, Heuss-Assbichler S (1997) Intracrystalline equilibria and immiscibility along the join clinzoisite-epidote: an experimental and ^{57}Fe Mössbauer study. *N Jb Miner Abh* 172: 43–67
- Fehr KT, Hobelsberger B (1997) Experimentelle Bestimmung der chemischen Potentiale von Hedenbergit in der Mischreihe Hedenbergit-Petedunnit. *Beiheft European J Miner* 9: 98
- Fehr KT, Huber AL (2001) Stability and phase relations of $\text{Ca}[\text{ZnSi}_3\text{O}_8]$, a new phase with feldspar structure in the system CaO-ZnO-SiO_2 . *Am Miner* 86: 21–28
- Grodzicki M, Heuss-Assbichler S, Amthauer G (2001) Mössbauer investigations and molecular orbital calculations on epidote. *Phys Chem Miner* 28: 675–681
- Gustafson WI (1974) The stability of andradite, hedenbergite and related minerals in the system Ca-Fe-Si-O-H . *J Petrol* 15: 455–496
- Hafner S, Huckenholz HG (1971) Mössbauer spectrum of synthetic Ferri diopside. *Nature* 233: 9–11
- Haselton HT, Robie RA, Hemingway BS (1987) Heat capacities of synthetic hedenbergite, ferrobustamite, and $\text{CaFeSi}_2\text{O}_6$ glass. *Geochim Cosmochim Acta* 51: 2211–2217
- Heuer M, Huber AL, Bromiley G (2002a) Crystal structure of calcium iron zinc catena-disilicate- $\text{Ca}_{0.98}\text{Fe}_{0.59}\text{Zn}_{0.46}\text{Si}_{1.98}\text{O}_6$. *Z Kristallogr New Crystal Structures* 217: 465–466
- Heuer M, Huber AL, Redhammer G (2002b) Crystal structure Calcium iron zinc catena-disilicate- $\text{Ca}_{1.00}\text{Fe}_{0.21}\text{Zn}_{0.85}\text{Si}_{1.97}\text{O}_6$. *Z Kristallogr New Crystal Structures* 217: 467–468
- Huber AL, Fehr KT (2002) Crystal chemistry and thermodynamic mixing properties of hedenbergite-petedunnite-johannsenite-diopside solid solutions. *EMPG 2002 J Conf Abstr* 7: 47
- Huckenholz HG, Lindhuber W, Springer J (1974) The join $\text{CaSiO}_3\text{-Al}_2\text{O}_3$ of the $\text{CaO-Al}_2\text{O}_3\text{-Fe}_2\text{O}_3\text{-SiO}_2$ quaternary system and its bearing on the formation of granditic garnets and fassaite pyroxenes. *N Jhb Miner Abh* 121: 160–207
- Huckenholz HG, Hölzl E, Lindhuber W (1975) Grossularite, its solidus and liquidus relations in the $\text{CaO-Al}_2\text{O}_3\text{-SiO}_2\text{-H}_2\text{O}$ system up to 10 kbar. *N Jhb Miner Abh* 124: 1–46
- Kawasaki T, Ito E (1994) An experimental determination of the exchange reaction of Fe^{2+} and Mg^{2+} between olivine and Ca-rich clinopyroxene. *Am Miner* 79: 461–477
- Kinrade J, Skippen GB, Wiles DR (1975) A Mössbauer observation on hedenbergite synthesis. *Geochim Cosmochim Acta* 39: 1325–1327
- Kühberger A, Fehr KT, Huckenholz HG, Amthauer G (1989) Crystal chemistry of a natural schorlomite and Ti-andradites synthesized at different oxygen fugacities. *Phys Chem Miner* 16: 734–740
- Lipka J, Petrik I, Toth I, Gajdosova M (1995) Mössbauer study of allanite. *Acta Physica Slovaca* 45: 61–66
- Luth WC, Tuttle OF (1963) Externally heated cold seal pressure vessels for use to 10 000 bars and 750 °C. *Am Mineral* 48: 1401–1403
- Moecher DP, Chou I-M (1990) Experimental investigation of andradite and hedenbergite equilibria employing the hydrogen sensor technique, with revised estimates of $\Delta_f G_{m,298}$ for andradite and hedenbergite. *Am Mineral* 75: 1327–1341
- Nakano T, Yoshino T, Shimazaki H, Shimizu M (1994) Pyroxene composition as an indicator in the classification of skarn deposits. *Econ Geol* 89: 1567–1580
- Nolan J (1969) Physical properties of synthetic and natural pyroxenes in the system diopside-hedenbergite-acmite. *Min Mag* 37: 216–229
- Ohashi H, Osawa T, Sato A, Tsukimura K (1996) Crystal structures of $(\text{Na,Ca})(\text{Sc,Zn})\text{Si}_2\text{O}_6$ clinopyroxenes formed at 6 GPa pressure. *J Min Petr Econ Geol* 91: 21–27
- Perkins D, Vielzeuf D (1992) Experimental investigation of Fe-Mg distribution between olivine and clinopyroxene: implications for mixing properties of Fe-Mg in clinopyroxene and garnet-clinopyroxene thermometry. *Am Mineral* 77: 774–783
- Pouchou L, Pichoir F (1984) A new model for quantitative X-ray microanalysis. Part I: Application to the analysis of homogeneous samples. *Rech Aerospac* 3: 13–38
- Raudsepp M, Hawthorne FC, Turnock AC (1990) Evaluation of the Rietveld method for the characterization of fine-grained products of mineral synthesis: the diopside-hedenbergite join. *Can Mineral* 28: 93–109
- Rutstein MS, Yund RA (1969) Unit-cell parameters of synthetic diopside-hedenbergite solid solutions *Am Mineral* 54: 238–245
- Redhammer G (1998) Mössbauer spectroscopy and Rietveld refinement on synthetic ferri-Tschermak's molecule $\text{CaFe}^{3+}(\text{Fe}^{3+}\text{Si})\text{O}_6$. *Eur J Mineral* 10: 439–452
- Redhammer G, Amthauer G, Lottermoser W, Treutmann W (2000) Synthesis and structural properties of clinopyroxenes of the hedenbergite $\text{CaFe}^{2+}\text{Si}_2\text{O}_6$ -aegirine $\text{NaFe}^{3+}\text{Si}_2\text{O}_6$ solid-solution series. *Eur J Miner* 12: 105–120
- Robinson K, Gibbs GV, Ribbe PH (1971) Quadratic elongation: a quantitative measure of distortion in coordination polyhedra. *Science* 172: 567–570
- Rothkopf AL, Fehr KT (1998) Stabilitäts- und Phasenbeziehungen von $\text{CaZnSi}_3\text{O}_8$ -einer neuen Phase mit Feldspatstruktur im System CaO-ZnO-SiO_2 . *Beiheft Eur J Mineral* 10: 242
- Sack R, Ghiorso MS (1994) Thermodynamics of multicomponent pyroxenes, I Formulation of a general model. *Contrib Mineral Petrol* 116: 277–286
- Schneider J, Young RA (1993) WYRIET3. Personal communication
- Shannon RD (1976) Revised effective ionic radii and systematic studies of interatomic distances in halides and chalcogenides. *Acta Crystallogr* A32: 751
- Tennant WC, McCammon CA, Miletich R (2000) Electric-field gradient and mean-squared-displacement tensors in hedenbergite from single-crystal Mössbauer milliprobe measurements. *Phys Chem Miner* 27: 156–163
- Turnock AC, Lindsley DH, Grover JE (1973) Synthesis and unit cell parameters of Ca-Mg-Fe pyroxenes. *Am Mineral* 58: 50–59
- Yoder HS (1950) High-low quartz inversion up to 10 000 bars. *Trans Am Geophys Union* 31: 827–835
- Zhang L, Ahsbahs H, Hafner SS, Koutoglu A (1997) Single-crystal compression and crystal structure of clinopyroxene up to 10 GPa. *Am Mineral* 82: 245–258